

Progressive Divide-and-Conquer via Subsampling Decomposition for Accelerated MRI

Chong Wang, Lanqing Guo, Yufei Wang, Hao Cheng, Yi Yu, Bihan Wen*

Nanyang Technological University, Singapore

{wangl711, lanqing001, yufei001, HAO006, yuyi0010, bihan.wen}@ntu.edu.sg

Abstract

Deep unfolding networks (DUN) have emerged as a popular iterative framework for accelerated magnetic resonance imaging (MRI) reconstruction. However, conventional DUN aims to reconstruct all the missing information within the entire null space in each iteration. Thus it could be challenging when dealing with highly ill-posed degradation, usually leading to unsatisfactory reconstruction. In this work, we propose a Progressive Divide-And-Conquer (PDAC) strategy, aiming to break down the subsampling process in the actual severe degradation and thus perform reconstruction sequentially. Starting from decomposing the original maximum-a-posteriori problem of accelerated MRI, we present a rigorous derivation of the proposed PDAC framework, which could be further unfolded into an end-to-end trainable network. Specifically, each iterative stage in PDAC focuses on recovering a distinct moderate degradation according to the decomposition. Furthermore, as part of the PDAC iteration, such decomposition is adaptively learned as an auxiliary task through a degradation predictor which provides an estimation of the decomposed sampling mask. Following this prediction, the sampling mask is further integrated via a severity conditioning module to ensure awareness of the degradation severity at each stage. Extensive experiments demonstrate that our proposed method achieves superior performance on the publicly available fastMRI and Stanford2D FSE datasets in both multi-coil and single-coil settings. Code is available at <https://github.com/ChongWang1024/PDAC>.

1. Introduction

Magnetic resonance imaging (MRI) is a widely used non-invasive imaging technique that provides detailed visualization of anatomical structures for medical diagnosis. MRI scanners sequentially collect data in the frequency domain, commonly referred to as k -space, from which MR images are reconstructed. One inherent limitation of MRI is the

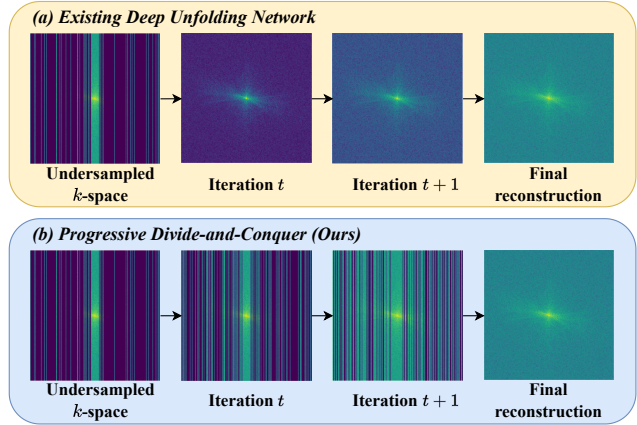


Figure 1. In each iteration: (a) Existing deep unfolding networks recover the information in the entire null space; (b) Our proposed method decomposes the entire null space and selectively retrieves information within specific segments of the null space, progressing from those that are easier to recover to more challenging ones.

protracted data acquisition time, which can cause patient discomfort and result in artifacts in the reconstructed images due to physiological movements during the acquisition. Thus accelerating the data acquisition process has been a primary focus in the MRI community. Compressed sensing (CS) [10, 22] is a common approach to accelerate the measurement acquisition process of MRI. These approaches employ undersampled data in k -space and exploit sparsity and incoherence to achieve accurate reconstructions. Specifically, traditional CS techniques necessitate that the underlying MR images exhibit sufficient sparsity in certain transform domains or learned dictionaries [29]. However, these assumptions can be overly restrictive for reconstructing MR images subjected to various degradations, limiting the performance of these traditional approaches.

Recent advancements in deep learning have demonstrated superior performance in MRI reconstruction by leveraging a large collection of training data [6, 8, 16, 31, 44]. Deep unfolding networks (DUN) [39, 43, 45], in particular, have emerged as a reliable framework for MRI reconstruction by unrolling an iterative optimization algorithm

*Bihan Wen is the corresponding author.

into an end-to-end trainable network. This approach establishes a potent deep framework that integrates explicit constraints based on the degradation model, offering a crucial foundation for effectively addressing ill-posed reconstruction problems. However, the efficacy of this constraint may be compromised, especially when solving highly ill-posed reconstruction problems, as it solely regularizes the limited range space of the sensing matrix. Figure 1 (a) shows one example in which a conventional DUN aims to reconstruct the full samples from the highly undersampled measurements in k -space in each iteration. Consequently, the reconstruction quality may degrade due to cumulative errors.

In this work, we present a novel iterative strategy, namely Progressive Divide-and-Conquer (PDAC), by decomposing the subsampling process in the actual severe degradation and thus performing reconstruction sequentially. Specifically, we initiate by reformulating the original maximum-a-posteriori problem of accelerated MRI in a way that the original severe problem can be progressively decoupled into a series of moderate corruptions. Accordingly, we present a rigorous derivation of the reconstruction process of PDAC, which is further unfolded into an end-to-end trainable network. With the merit of degradation decomposition, each iteration in PDAC focuses solely on retrieving the information within the specific parts of null space, specifically targeting a particular moderate degradation according to the decomposition, as shown in Figure 1 (b). Besides, such decomposition is adaptively learned as an auxiliary task throughout the PDAC iterations. Specifically, a degradation predictor is adopted to predict the subsampling mask that characterizes the decomposed degradation process. This learning-to-decompose mechanism serves to guide the preservation of specific reconstructed information, concurrently discarding inaccuracies. Consequently, each intermediate reconstruction is characterized by a specific degradation severity, as indicated by the predicted subsampling mask. Thus we further introduce an embedding module to guarantee awareness of the degradation severity at each iterative stage. Experimental results show that the proposed method can achieve superior performance consistently in both single-coil and multi-coil MRI reconstruction on the fastMRI and Stanford2D FSE datasets.

The main contributions of this work are as follows:

- We propose the Progressive Divide-and-Conquer (PDAC) method for accelerated MRI, a novel iterative strategy that decomposes the subsampling process of severe degradation into a series of moderate ones and then performs reconstruction sequentially. In PDAC, each iteration is dedicated to recovering a specific decomposed degradation.
- We unfold the PDAC iterations into an end-to-end trainable network, simultaneously incorporating the learning of degradation decomposition as an auxiliary task.

To guarantee awareness of decomposed degradation at each iteration, we introduce a severity embedding module, facilitating the integration of the decomposed subsampling mask into our network.

- Extensive experimental results on the fastMRI and Stanford2D FSE datasets in both single-coil and multi-coil MRI reconstruction show that the proposed PDAC achieves superior performance compared to the state-of-the-art.

2. Related Work

2.1. Accelerated MRI

The success of reconstructing images in CS-MRI relies on incorporating an additional regularizer capturing assumed image priors due to its ill-posed nature. Traditional methods commonly employ handcrafted priors such as total variation [23] and low-rankness [20] to regulate the reconstruction results. In addition to these approaches, dictionary learning [28] stands out as a more flexible method for MRI reconstruction, directly learning an adaptive sparse representation from the data. More recently, deep learning-based methods [3, 12, 25, 26, 37, 38] have achieved remarkable performance in MRI reconstruction. CDF-Net [26] introduces a cross-domain fusion network for MRI reconstruction by exploiting the relationship in both frequency and spatial domains. Specifically, model-based learning methods have emerged as a popular paradigm for solving MRI reconstruction. For example, ADMM-Net [39] attempts to learn the parameters of the data flow in the alternating direction method of multipliers (ADMM) algorithm and has demonstrated superior results for MRI reconstruction.

2.2. Deep Unfolding Networks

By unfolding deep networks that embody the steps from existing model-based iterative algorithms and optimizing in an end-to-end manner, DUN has demonstrated promising performance on various inverse problems, such as super-resolution [43, 45] and deblurring [18, 24]. DUN also becomes a predominant approach for solving MRI reconstruction [4, 17, 39, 40] that ensures the consistency of the predictions with respect to the degradation model. The earliest unrolling method can be traced back to LISTA [13] where the authors propose to unfold the iterative shrinkage thresholding algorithm (ISTA) [5] for sparse coding. MoDL [2] introduces a model-based learning framework by unfolding a weight-sharing network with several iterations, thus offering appealing performance with less computational cost. [46] exploits dual domain priors on both image space and k -space to simultaneously constrain the MRI reconstruction results via a customized dual domain recurrent network. However, existing unfolding methods aim to recover the information in the entire null space at each stage, which can

lead to inaccurate reconstructions, particularly when dealing with highly degraded problems. In this paper, we introduce a novel unfolded paradigm that decomposes the degradation and progressively retrieves specific segments of the null space, targeting a particular decomposed degradation.

3. Preliminary

3.1. MRI Acquisition

Compressed sensing MRI accelerates the data acquisition process by collecting less data than the Nyquist rate in the k -space. The MR image is reconstructed by maximum a posteriori (MAP) problem, involving the data fidelity term and regularizer $\Psi(\cdot)$, which is

$$\min_{\mathbf{x}} \|\mathbf{y} - A\mathbf{x}\|_2^2 + \lambda \Psi(\mathbf{x}), \quad (1)$$

where $\mathbf{x} \in \mathbb{C}^n$ denotes the underlying spatial ground truth image, $\mathbf{y} \in \mathbb{C}^n$ is the zero-filled undersampled measurements, $A \in \mathbb{C}^{n \times n}$ denotes the degradation process and λ is the weighting parameter that controls the penalty strength of the regularizer.

Single-coil MRI. In single-coil MRI, the degradation process corresponds to subsampling in the k -space

$$\mathbf{y} = A\mathbf{x} + \epsilon = D\mathcal{F}\mathbf{x} + \epsilon, \quad (2)$$

where $D = \text{diag}(\mathbf{d}) \in \mathbb{R}^{n \times n}$, $\mathbf{d} \in \{0, 1\}^n$ is a diagonal sampling matrix characterizing the sampled location in k -space, $\mathcal{F} \in \mathbb{C}^{n \times n}$ denotes the two-dimensional Fourier transform and $\epsilon \in \mathbb{C}^n$ is the measurement noise during the acquisition process. The ill-posedness stems from the underdetermination of D (i.e., $\text{rank}(D) = m \ll n$).

Multi-coil MRI. In the multi-coil MR system with C coils, the undersampled measurement obtained by the c th coil can be formulated as

$$\mathbf{y}_c = D\mathcal{F}S_c\mathbf{x} + \epsilon_c, \quad c = 1, \dots, C, \quad (3)$$

where the coil-sensitivity map $S_c \in \mathbb{C}^{n \times n}$ is a matrix encoding the sensitivity of the c -th coil. The coil-sensitivity map is usually normalized such that $\sum_{c=1}^C S_c^H S_c = I$.

3.2. Half Quadratic Splitting

Optimization problem (1) can be solved using variable splitting techniques such as half-quadratic splitting [1] by introducing an auxiliary variable \mathbf{z} , that reformulates (1) as

$$\min_{\mathbf{z}, \mathbf{x}} \|\mathbf{y} - A\mathbf{z}\|_2^2 + \mu \|\mathbf{z} - \mathbf{x}\|_2^2 + \lambda \Psi(\mathbf{x}), \quad (4)$$

where μ is the penalty parameter of the Lagrangian term. Then it can be solved using alternating minimization between two sub-problems as

$$\mathbf{z}_t = \underset{\mathbf{z}}{\text{argmin}} \|\mathbf{y} - A\mathbf{z}\|_2^2 + \mu \|\mathbf{z} - \mathbf{x}_{t-1}\|_2^2, \quad (5)$$

$$\mathbf{x}_t = \underset{\mathbf{x}}{\text{argmin}} \mu \|\mathbf{x} - \mathbf{z}_t\|_2^2 + \lambda \Psi(\mathbf{x}). \quad (6)$$

Note that (5) is a least-squares problem with a quadratic penalty term which has a closed-form solution, commonly dubbed as the data consistency step. The update process of \mathbf{x}_t corresponds to a Gaussian denoising problem that can be solved using any denoiser. By adopting a deep network as the regularizer in (6), the above iterative steps can be unfolded into an end-to-end trainable framework that is alternatively optimized between (5) and (6).

4. Method

Recovering the degradation A directly poses significant challenges, especially when $m \ll n$. To this end, we introduce the progressive divide-and-conquer (PDAC) algorithm, which initiates by breaking down a severe degradation into a series of moderate corruptions and recovering each decomposed degradation sequentially. Subsequently, we unfold the PDAC iterations into an end-to-end trainable network while simultaneously learning the degradation decomposition as an auxiliary task during the iteration. The overall framework of PDAC is illustrated in Figure 2.

4.1. Decomposing the Subsampling

The zero-filled degradation A can be decoupled into two parts as $A = D\mathcal{F}$. Specifically, D indicates the sampling matrix where the ill-posedness comes from since D is underdetermined. We can decompose such severe degradation caused by subsampling D into a product of multiple moderate degradations as

$$D = D_0 \cdots D_T = D_0 \cdots D_{t-1} \bar{D}_t \quad (7)$$

where $D_t = \text{diag}(\mathbf{d}_t)$, $\mathbf{d}_t \in \{0, 1\}^n$ is the decomposed diagonal sampling matrix and $\bar{D}_t = (\prod_{i=t}^T D_i)$. Specifically, $\text{rank}(\bar{D}_t) < \text{rank}(\bar{D}_{t+1})$, $\bar{D}_T = I$. Let $A_t = \bar{D}_t \mathcal{F}$ and we have $A_0 = A$, $A_T = \mathcal{F}$. Since the ill-posed nature of the problem only stems from the sampling matrix D , we now present a formal definition of the degradation severity of A_t according to the range space of its corresponding \bar{D}_t .

Definition 1. (Degradation severity). The degradation A_t is more severe when the range space of the sampling matrix \bar{D}_t^\top is a subspace of that in $A_{t'}$. According to the decomposition in (7), we have

$$\begin{aligned} \text{R}(\bar{D}_t^\top) \subset \text{R}(\bar{D}_{t'}^\top) \subset \text{R}(\bar{D}_T^\top) = \mathbb{R}^n, \quad \forall t < t' < T, \\ \text{R}(A_t^H) \subset \text{R}(A_{t'}^H) \subset \text{R}(A_T^H) = \mathbb{C}^n, \quad \forall t < t' < T. \end{aligned} \quad (8)$$

This decomposition provides a means of disentangling severe corruption into a series of moderate ones. Following this, we will introduce a progressive divide-and-conquer strategy, addressing the original severe degradation problem iteratively through degradation decomposition.

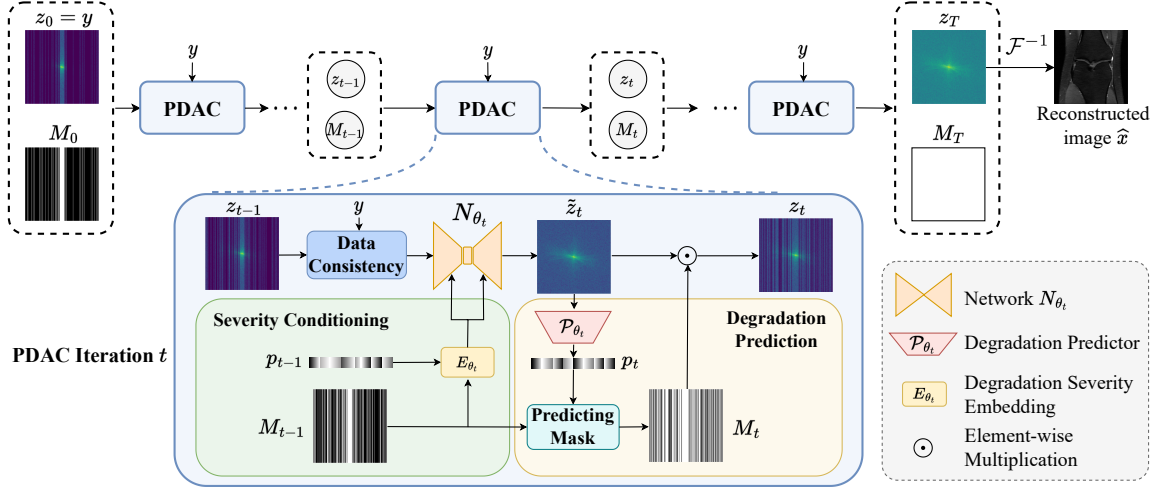


Figure 2. Illustration of the proposed *progressive divide-and-conquer (PDAC)* framework, where the iterative process is detailed in Algorithm 1. Each iteration consists of data consistency, network reconstruction, and degradation using M_t . Besides, the network learns the decomposed degradation, characterized by M_t , as an auxiliary task along iterations via (1) Degradation Prediction: we adaptive learn a decomposed sampling mask M_t which indicates the frequency components to preserve in \tilde{z}_t ; (2) Severity Conditioning: we adopt a severity embedding module E_{θ_t} to guarantee awareness of the degradation pattern in M_{t-1} .

4.2. Progressive Divide-and-Conquer

Solving (1) with a single regularizer can be challenging when the measurement \mathbf{y} is significantly degraded. Alternatively, we propose to find a solution by introducing a series of regularizers according to the decomposed degradation defined in (7), and the problem can be reformulated as

$$\min_{\mathbf{x}} \|\mathbf{y} - A_0 \mathbf{x}\|_2^2 + \sum_{t=1}^T \lambda_t \Psi_t(A_t \mathbf{x}), \quad (9)$$

where $\{\Psi_t(A_t \mathbf{x})\}_{t=1}^T$ are the regularizers encapsulating the prior knowledge on the distribution of less degraded measurements $A_t \mathbf{x}$ and λ_t is the weighting parameter accordingly. (9) can be solved by adopting variable splitting algorithms such as half-quadratic splitting (HQS) [1]. Specifically, we can write the augmented Lagrangian form of (9) by introducing an auxiliary variable $\mathbf{z}_1 = A_1 \mathbf{x}$ as:

$$\begin{aligned} \min_{\mathbf{z}_1, \mathbf{x}} & \|\mathbf{y} - D_0 \mathbf{z}_1\|_2^2 + \mu_1 \|\mathbf{z}_1 - A_1 \mathbf{x}\|_2^2 + \lambda_1 \Psi_1(\mathbf{z}_1) \\ & + \sum_{t=2}^T \lambda_t \Psi_t(A_t \mathbf{x}), \quad \text{s.t. } \mathbf{z}_1 \in \mathbb{R}(A_1^H). \end{aligned} \quad (10)$$

The constraint implies that the intermediate measurement \mathbf{z}_1 should lie in the range space of decompose degradation A_1 , as indicated by the Lagrangian term $\|\mathbf{z}_1 - A_1 \mathbf{x}\|_2^2$. Then it can be decoupled into two sub-problems as

$$\begin{aligned} \mathbf{z}_1 = \operatorname{argmin}_{\mathbf{z}_1} & \|\mathbf{y} - D_0 \mathbf{z}_1\|_2^2 + \mu_1 \|\mathbf{z}_1 - A_1 \mathbf{x}\|_2^2 \\ & + \lambda_1 \Psi_1(\mathbf{z}_1), \quad \text{s.t. } \mathbf{z}_1 \in \mathbb{R}(A_1^H) \end{aligned} \quad (11)$$

$$\min_{\mathbf{x}} \mu_1 \|\mathbf{z}_1 - A_1 \mathbf{x}\|_2^2 + \sum_{t=2}^T \lambda_t \Psi_t(A_t \mathbf{x}). \quad (12)$$

Problem (9) characterized by the degradation A_0 is now converted to a less severe problem (12) characterized by A_1 via introducing an intermediate measurement \mathbf{z}_1 . Solving the sub-problem in (11) can be interpreted as recovering the information loss during the decomposed subsampling D_0 , thus transforming the optimization problem into a less severe one.

Unfortunately, directly solving (12) could still be challenging. One can perform a similar variable splitting by introducing variable $\mathbf{z}_2 = A_2 \mathbf{x}$ that splits (12) into another two sub-problems via updating \mathbf{z}_2 and \mathbf{x} . In this case, the overall optimization problem (9) could be approximated via solving three variables, $\mathbf{z}_1, \mathbf{z}_2$ and \mathbf{x} , sequentially. Towards this end, such a variable splitting trick can be performed progressively by introducing a series of auxiliary variables $\{\mathbf{z}_t = A_t \mathbf{x}\}_{t=1}^T$, leading to solving sequential sub-problems $\{\mathbf{z}_1, \dots, \mathbf{z}_t\}$ and \mathbf{x} as

$$\begin{aligned} \mathbf{z}_\tau = \operatorname{argmin}_{\mathbf{z}_\tau \in \mathbb{R}(A_\tau^H)} & \mu_{\tau-1} \|\mathbf{z}_{\tau-1} - D_{\tau-1} \mathbf{z}_\tau\|_2^2 \\ & + \mu_\tau \|\mathbf{z}_\tau - A_\tau \mathbf{x}\|_2^2 + \lambda_\tau \Psi_\tau(\mathbf{z}_\tau), \quad \forall \tau \in [1, t], \end{aligned} \quad (13)$$

$$\min_{\mathbf{x}} \mu_t \|\mathbf{z}_t - A_t \mathbf{x}\|_2^2 + \sum_{i=t+1}^T \lambda_i \Psi_i(A_i \mathbf{x}). \quad (14)$$

Note that the final estimation \mathbf{x} only updates once, after we have sequentially solved intermediate variables $\{\mathbf{z}_1, \dots, \mathbf{z}_T\}$. The final reconstruction result $\hat{\mathbf{x}}$ after progressive splitting could be obtained according to \mathbf{z}_T as

$$\hat{\mathbf{x}} = \operatorname{argmin}_{\mathbf{x}} \mu_T \|\mathbf{z}_T - \mathcal{F} \mathbf{x}\|_2^2, \quad (15)$$

which has a simple closed-form solution via directly taking the inverse Fourier transform as $\hat{\mathbf{x}} = \mathcal{F}^{-1} \mathbf{z}_T$.

Now the problem lies in the solution of each intermediate auxiliary measurement \mathbf{z}_t . The update process of variable \mathbf{z}_t in (13) can be reformulated by merging the squares as

$$\begin{aligned} \mathbf{z}_t &= \operatorname{argmin}_{\mathbf{z}_t \in \mathbb{R}(A_t^H)} \|U_t \mathbf{z}_t - \mathbf{v}_t\|_2^2 + \lambda_t \Psi_t(\mathbf{z}_t), \\ \text{where } U_t^\top U_t &= \mu_{t-1} D_{t-1}^\top D_{t-1} + \mu_t I, \\ U_t^\top \mathbf{v}_t &= \mu_{t-1} D_{t-1}^\top \mathbf{z}_{t-1} + \mu_t A_t \mathbf{x}. \end{aligned} \quad (16)$$

Note that $U_t^\top U_t = \operatorname{diag}(\mathbf{u}_t)$, $\mathbf{u}_t \in \{\mu_{t-1}, \mu_{t-1} + \mu_t\}^n$ is a diagonal matrix which is easily invertible. Thus it is equivalent to solve

$$\mathbf{z}_t = \operatorname{argmin}_{\mathbf{z}_t \in \mathbb{R}(A_t^H)} \|\mathbf{z}_t - U_t^{-1} \mathbf{v}_t\|_{U_t^\top U_t}^2 + \lambda_t \Psi_t(\mathbf{z}_t), \quad (17)$$

where $\|\cdot\|_{U_t^\top U_t}^2$ is the weighted Euclidean norm [7] according to the diagonal of $U_t^\top U_t$. From a Bayesian perspective, the optimization in (17) corresponds to a denoising problem with noisy input $U_t^{-1} \mathbf{v}_t$, which can be implicitly solved with neural networks. Thus, the subproblem in (13) can be solved in three steps: 1) Calculate $U_t^{-1} \mathbf{v}_t$ which essentially performs data consistency on the results from the previous reconstruction \mathbf{z}_{t-1} ; 2) Obtain a denoising result via a neural network N_{θ_t} ; 3) Projection onto the range space of the decomposed degradation $\mathbb{R}(A_t^H)$.

Finally, the overall optimization problem in (9) can be solved by breaking down the original severe degradation A and reconstructing each decomposed degradation D_t accordingly. The whole iterative paradigm is described in Algorithm 1, dubbed *progressive divide-and-conquer*. The final reconstruction result can be obtained by unfolding the proposed iterations into an end-to-end trainable network.

4.3. Learning to Decompose

So far, we have derived the proposed progressive divide-and-conquer framework based on the subsampling decomposition, which provides an indication of designing the data flow of our unfolded network. An important question that arises is: *how to obtain such a set of decomposed degradation $\{A_t\}_{t=1}^T$ based on the original degradation process A ?* Ideally, a straightforward solution is to jointly optimize such decomposition together in P_1 , that is

$$\min_{\mathbf{x}, \{A_t\}_{t=1}^T} \|\mathbf{y} - A_0 \mathbf{x}\|_2^2 + \sum_{t=1}^T \lambda_t \Psi_t(A_t \mathbf{x}). \quad (18)$$

Unfortunately, the exact determination of such a decomposition set in (18) proves to be an NP-hard problem [34]. A remedy to the above problem is to gradually predict the decomposed degradation along with the PDAC iteration. Specifically, a degradation predictor is introduced to estimate a sampling matrix \bar{D}_t that characterizes the decomposed degradation A_t based on the current reconstruction

Algorithm 1 Progressive Divide-And-Conquer (PDAC)

Input: $\mathbf{y}, \mu_t, \mathcal{N}_{\theta_t}, A_t = \bar{D}_t \mathcal{F}$ defined in Section 4.1.

Initialization: $\mathbf{z}_0 = \mathbf{y}, \mathbf{x} = \mathcal{F}^{-1} \mathbf{y}$

for $t = 1, \dots, T$ **do**

$$U_t^\top U_t = \mu_{t-1} D_{t-1}^\top D_{t-1} + \mu_t I$$

$$U_t^\top \mathbf{v}_t = \mu_{t-1} D_{t-1}^\top \mathbf{z}_{t-1} + \mu_t A_t \mathbf{x}$$

$$\mathbf{z}'_t = U_t^{-1} \mathbf{v}_t \quad \# \text{ data consistency}$$

$$\tilde{\mathbf{z}}_t = N_{\theta_t}(\mathbf{z}'_t) \quad \# \text{ reconstruction}$$

$$\mathbf{z}_t = \bar{D}_t \tilde{\mathbf{z}}_t \quad \# \text{ degradation}$$

end for

$$\hat{\mathbf{x}} = \mathcal{F}^{-1} \mathbf{z}_T$$

return $\hat{\mathbf{x}}$

$\tilde{\mathbf{z}}_t$. The degradation step in each iteration can be interpreted as retaining well-reconstructed frequency in the k -space while discarding the inaccurate information. Following Definition 1, the severity of the decomposed degradation becomes weaker as t increases. Accordingly, \bar{D}_t tends to preserve more restored frequency as the reconstruction becomes more reliable with iterations until $\bar{D}_T = I$.

Predicting subsampling mask. In the context of MRI, the sampling matrix refers to a subsampling mask M in the k -space. Specifically, we consider the Cartesian mask (e.g., as shown in Figure 2), which is the most commonly used in accelerated MRI. The Cartesian mask corresponds to selecting frequency columns in the k -space. Thus, it can be represented by a binary vector \mathbf{m} indicating the location of selected frequency sub-bands, i.e., $M = \mathbf{m} \mathbf{1}^\top$, with $\mathbf{1}$ represents an all-one vector. Following Definition 1, the subsampling mask should fulfill two properties: 1) the number of the sampled frequency columns should increase with iteration until a full mask; 2) the location of the sampled frequency columns should encompass the previous one.

Consequently, we propose to predict subsampling mask \mathbf{m}_t conditioned on the current reconstruction $\tilde{\mathbf{z}}_t$ and previous mask \mathbf{m}_{t-1} . To make it feasible for network learning, we pre-define a budget $b_t = \|\mathbf{m}_t\|_0$ that restricts the number of sampled frequency columns in each mask \mathbf{m}_t , allowing the network to learn the frequency column locations within \mathbf{m}_t . In detail, a degradation predictor \mathcal{P}_{θ_t} is introduced to estimate a probability \mathbf{p}_t indicating the location of frequency columns to sample, i.e., $\mathbf{p}_t = \mathcal{P}_{\theta_t}(\tilde{\mathbf{z}}_t)$. Thus, the \mathbf{m}_t can be obtained via adding extra frequency columns, selected from the $b_t - b_{t-1}$ largest probability of \mathbf{p}_t , on the previous mask \mathbf{m}_{t-1} . For each index i

$$\mathbf{m}_t^{[i]} = \mathbf{m}_{t-1}^{[i]} + \mathbb{I}(i \in \operatorname{idx}) \quad \forall i, \quad (19)$$

where idx is the indices of the $b_t - b_{t-1}$ largest values in $\mathbf{p}_t \odot (1 - \mathbf{m}_{t-1})$ with \odot denotes the Hadamard product.

Setting	b_0, \dots, b_T ($T = 8$)
Multi-coil 8×	[48, 192, 288, 320, 336, 352, 364, 376, 384]
Single-coil 8×	[40, 160, 240, 264, 280, 292, 304, 312, 320]
Single-coil 4×	[80, 160, 240, 264, 280, 292, 304, 312, 320]

Table 1. The sampling budget schedule for each experiment.

Decomposed degradation loss. Ideally, the predicted probability \mathbf{p}_t shall indicate the confidence on the corresponding frequency columns in $\tilde{\mathbf{z}}_t$. We define such confidence concerning the normalized reconstruction error in each frequency column. In detail, given the k -space ground truth Y_{gt} , the normalized reconstruction error \mathbf{e}_t is given by

$$\mathbf{e}_t = \frac{\mathbf{1}^\top \tilde{\mathbf{Z}}_t - \mathbf{1}^\top Y_{gt}}{\mathbf{1}^\top Y_{gt}}. \quad (20)$$

Then we convert the range of \mathbf{e}_t into $[0, 1]$ as a reference of probability \mathbf{p}_t , *i.e.*, $\hat{\mathbf{e}}_t = 2 \times \text{Sigmoid}(|\mathbf{e}_t|) - 1$, where $|\mathbf{e}_t|$ denotes element-wise absolute value of \mathbf{e}_t . Building upon this, we introduce a decomposed degradation loss between \mathbf{p}_t and $1 - \hat{\mathbf{e}}_t$ using ℓ_1 -norm as:

$$\mathcal{L}_{prob} = \sum_t^T \|\mathbf{m}_t \odot (\mathbf{p}_t - (1 - \hat{\mathbf{e}}_t))\|_1. \quad (21)$$

Degradation severity conditioning. During each iteration of PDAC, the network aims to reconstruct an intermediate measurement from a specific degradation severity, *i.e.*, $\mathbf{z}_t \in \mathbb{R}(A_t^H)$. Thus we further adopt a severity conditioning module E_{θ_t} to guarantee awareness of the degradation pattern in the k -space. Rather than directly conditioning on the binary mask vector \mathbf{m}_t , we propose to embed the masked confidence $\mathbf{m}_t \odot \mathbf{p}_t$ to further incorporate the estimated probability on each sampled frequency column. Motivated by [27], we conduct an adaptive layer norm (adaLN) for inserting the information of the degradation severity.

4.4. Training Objectives

The iteration of PDAC is unfolded into a trainable network and optimized in an end-to-end manner. To optimize the final reconstruction result, following the previous works [14, 15, 41], we adopt the ℓ_1 -norm pixel-wise loss $\mathcal{L}_{rec} = \|\hat{X} - X_{gt}\|_1$. The total loss is defined as follows

$$\mathcal{L}_{total} = \mathcal{L}_{rec} + \alpha \mathcal{L}_{prob}, \quad (22)$$

where α denotes the balancing parameter.

5. Experiments

5.1. Experimental Setups

Dataset. The experiments are conducted on the fastMRI dataset [42] and Stanford2D FSE dataset [9]. For the fastMRI dataset, we run the experiments on both the single-coil and multi-coil knee data which consists of 1,172

Dataset	Method	PSNR↑	SSIM↑	NMSE↓	
fastMRI knee	Zero-filled	27.42	0.7000	0.0704	
	ESPIRiT [35]	28.20	0.5965	0.1442	
	U-Net [30]	34.18	0.8601	0.0151	
	E2E-VarNet [32]	36.81	0.8873	0.0090	
	HUMUSNet [12]	36.84	0.8879	0.0092	
	HUMUSNet* [12]	37.03	0.8933	0.0090	
	HUMUSNet+PDAC	37.12	0.8905	0.0085	
Stanford2D	Zero-filled	29.24	0.7175	0.0948	
	U-Net [30]	33.77	0.8953	0.0333	
	E2E-VarNet [32]	36.48	0.9220	0.0172	
	HUMUSNet [12]	35.43	0.9134	0.0219	
		HUMUSNet+PDAC	36.77	0.9247	0.0166

Table 2. The quantitative results of 8× accelerated multi-coil MRI reconstruction using our proposed model and recent methods on the fastMRI knee and Stanford 2D datasets. (*) denotes the model takes extra adjacent slices in the input.

complexed-value MRI scans with 973 scans for training and 199 scans for validation. Each scan approximately provides 30-40 coronal cross-sectional knee slices.

Mutil-coil track: Each slice in the MRI scans is sampled by a total $C = 15$ coils and each slice is center cropped into a size of 384×384 . Following the previous setting [12, 32], we conduct the reconstruction on 8× accelerated MRI, with a central fraction of 4% on low-frequency sub-bands.

Single-coil track: Following [14, 15], all images are center cropped into a size of 320×320 . We reconstruct MR images at two acceleration factors of 4× and 8×, with a central fraction of 8% and 4% on low-frequency, respectively.

We also run experiments of multi-coil reconstruction on the Stanford2D FSE dataset, which consists of 89 fully-sampled volumes. Following [12], we randomly sampled 80% data for training and used the rest for validation. We conduct the reconstruction on 8× accelerated MRI that central cropped into a size of 384×384 .

Implementation details. The proposed method is implemented on PyTorch using NVIDIA RTX 4090 GPUs. We adopt the HUMUSNet [12] as the network backbone for our proposed PDAC framework. The original HUMUSNet [12] takes a central slice together with two adjacent slices as the input for reconstruction, while we follow the common setting that only uses a single slice as the input for a fair comparison with the existing methods. The detailed structures of degradation predictor \mathcal{P}_{θ_t} and severity conditioning module E_{θ_t} are provided in the supplementary material. The network is trained in an end-to-end manner with \mathcal{L}_{total} and optimized using AdamW [21]. We train the network with a learning rate of 0.0001 for 50 and 40 epochs on the multi-coil and single-coil settings, respectively, dropped by a factor of 10 at the last 5 epochs. Following [12], we set the total iteration step $T = 8$ and we customize the column budget $\{b_t\}$ increasing in a coarse-to-fine manner, as detailed in Table 1. The weight for the probability loss α is set to 0.01.

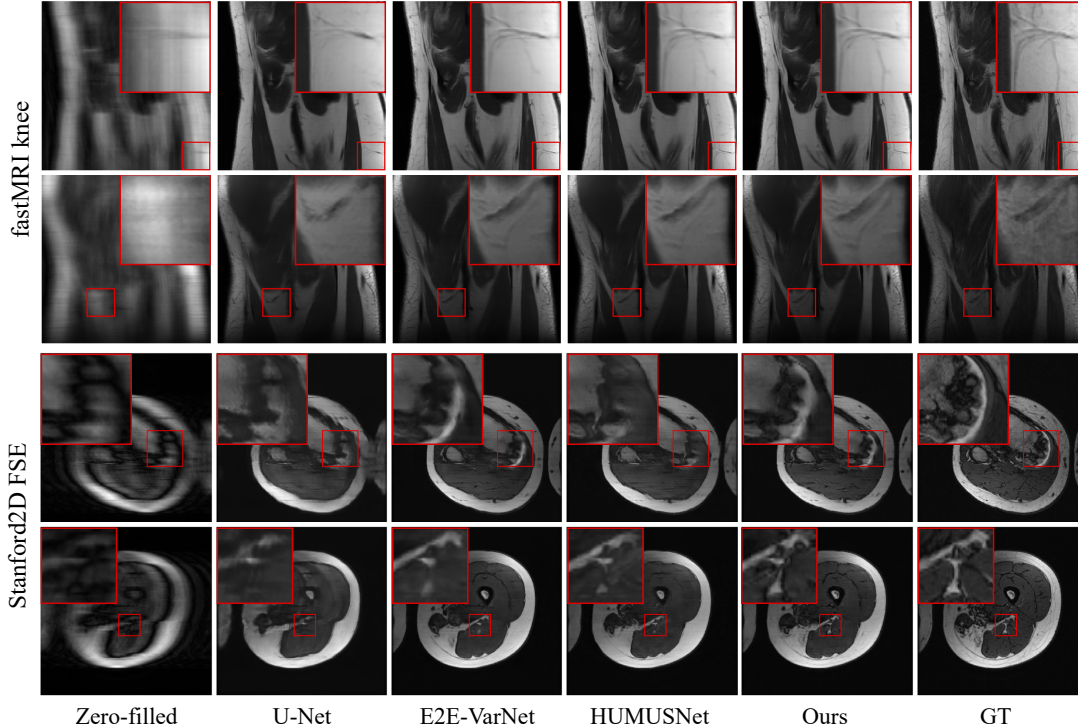


Figure 3. Examples of multi-coil accelerated MRI reconstruction results of zero-filled input, U-Net [30], E2E-VarNet [32], HUMUSNet [12], Ours and ground truth on the fastMRI [42] knee and Stanford2D FSE [9] datasets. Please zoom in to see the details.

5.2. Comparison with State-of-the-Art

To evaluate the performance of our proposed PDAC strategy, we make a comparison with several state-of-the-art methods in both multi-coil and single-coil settings. For the multi-coil setting, we adopt ESPIRiT [35], U-Net [30], E2E-VarNet [32] and HUMUSNet [12] as the competing methods for $8\times$ accelerated MRI reconstruction. Note that HUMUSNet* indicates the results of the model using extra adjacent slices as the input for reconstruction. For the single-coil setting, we compared the proposed methods with one classical method, *i.e.*, compressed sensing (CS) [33] and eight learning-based methods, *i.e.*, U-Net [30], KIKI-Net [11], Kiu-net [36], SwinIR [19], D5C5 [31], OUCR [14], ReconFormer [15] and HUMUSNet [12] on $4\times$ and $8\times$ accelerated reconstruction.

Tables 2 and 3 show the quantitative results of the multi-coil and single-coil MRI reconstruction, respectively. It is clear that our method can achieve superior performance consistently in both settings. For the multi-coil reconstruction in Table 2, the classical method ESPIRiT [35] adopts a hand-crafted total variation regularizer that encourages sparsity, which is too restrictive for reconstructing details in the image. Compared to the most recent method HUMUSNet [12], the proposed PDAC method can improve the PSNR from 36.84dB to 37.12dB using the same network backbone. Specifically, our method can even achieve

a better PSNR with comparable SSIM results compared to HUMUSNet* which uses extra information from adjacent MR slices in the input. For the Stanford2D FSE dataset, our method significantly improves the PSNR for 1.34dB compared to the HUMUSNet baseline. A similar trend can also be observed in the single-coil setting, where the proposed model establishes new state-of-the-art in terms of both PSNR and SSIM in $8\times$ reconstruction.

To further demonstrate the advantage of our method against other competing baselines, Figure 3 presents the visual examples of multi-coil MRI reconstruction results on fastMRI knee and Stanford2D FSE datasets. Our method excels in restoring MR images with enhanced details, particularly evident in the Stanford2D FSE dataset. Notably, HUMUSNet [12] fails to recover tissue structures, as illustrated in the third row of Figure 3, whereas our PDAC framework successfully restores the boundaries. In the bottom row of Figure 3, our method stands out as the sole approach that could restore a clear white triangle region, while other methods yield results plagued by blurry artifacts.

5.3. Ablation Study

To investigate the effectiveness of each key component of the proposed method, we perform experiments on several model variants on the Stanford2D FSE dataset.

The effect of degradation prediction. We introduce adaptive learning for degradation decomposition in conjunction

Method	4× acceleration		8× acceleration	
	PSNR↑	SSIM↑	PSNR↑	SSIM↑
Zero-filled	29.49	0.6541	26.84	0.5500
CS [33]	29.54	0.5736	26.99	0.4870
U-Net [30]	31.88	0.7142	29.78	0.6424
KIKI-Net [11]	31.87	0.7172	29.27	0.6355
Kiu-net [36]	32.06	0.7228	29.86	0.6456
SwinIR [19]	32.14	0.7213	30.21	0.6537
D5C5 [31]	32.25	0.7256	29.65	0.6457
OUCR [14]	32.61	0.7354	30.59	0.6634
ReconFormer [15]	32.73	0.7383	30.89	0.6697
HUMUSNet [12]	32.37	0.7221	31.04	0.6722
HUMUSNet+PDAC	32.73	0.7376	31.16	0.6739

Table 3. The quantitative results of 4× and 8× accelerated single-coil MRI reconstruction using our proposed model and recent methods on the fastMRI knee dataset.

with the PDAC iterations. However, one simple way to obtain such a decomposition is directly synthesizing each decomposed degradation based on the pre-defined budget b_t . Thus we conduct an ablation study by comparing to the PDAC model with random decomposed degradation. Specifically, the number of the frequency columns in m_t satisfies the same budget b_t but the location of the frequency columns is randomly sampled from a uniform distribution. However, the results indicate a significant degradation in performance, with a drop of approximately 0.31dB in PSNR, compared to our proposed learning-to-decompose strategy, as shown in Table 4. Our method predicts decomposed degradations based on the current reconstruction, akin to adaptively selecting well-recovered frequency components at each iteration. This progressive restoration of missing information in k -space unfolds gradually, from those that are easier to recover to more challenging ones.

The effect of decomposed degradation loss. Following the aforementioned learning-to-decompose strategy, a probability p_t is estimated from a degradation predictor \mathcal{P}_{θ_t} to indicate the confidence of each reconstruction frequency column. Such confidence is further regularized according to the normalized reconstruction error via the proposed decomposed degradation loss \mathcal{L}_{prob} . In order to illustrate the effectiveness of the decomposed degradation loss, we further conduct an experiment by training the PDAC model without \mathcal{L}_{prob} . The results, detailed in Table 4, reveal a drop in PSNR from 36.77dB to 36.48dB, underscoring the contribution of the decomposed degradation loss to the learning of the degradation predictor.

The effect of degradation severity conditioning. In the iteration of PDAC, the intermediate results are constrained to a specific subspace characterized by each decomposed sampling mask. To ensure an awareness of the degradation pattern, we introduce a severity conditioning module E_{θ_t} that integrates the information of masked confidence, denoted as $m_t \odot p_t$. To investigate the effectiveness of this condition-

Model	PSNR↑	SSIM↑	NMSE↓
HUMUSNet baseline	35.43	0.9134	0.0219
PDAC w/o degradation prediction	36.46	0.9233	0.0176
PDAC w/o degradation loss \mathcal{L}_{prob}	36.48	0.9238	0.0176
PDAC w/o severity conditioning	36.66	0.9241	0.0168
PDAC (Complete model)	36.77	0.9247	0.0166

Table 4. Ablation study to verify the effectiveness of each component in our method on the Stanford2D FSE dataset.

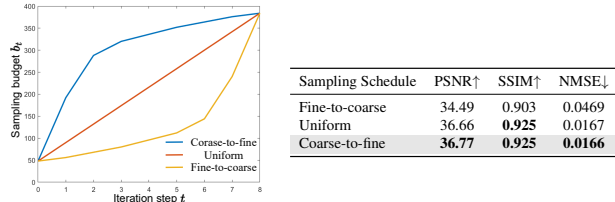


Figure 4. Ablation study on different sampling budget schedules.

ing module, we further conduct experiments by removing E_{θ_t} in the PDAC iteration, leading to a deterioration in performance compared to our complete framework.

The effect of sampling budget schedule. We conduct experiments on various schedules of the sampling budget b_t , including coarse-to-fine, uniform, and fine-to-coarse schedules. Figure 4 shows that coarse-to-fine scheduling yields the best performance in our PDAC iteration. This aligns with the design of PDAC, which aims to progressively recover the entire null space, moving from easier to more challenging aspects. The inherent suitability of coarse-to-fine scheduling for PDAC is evident, facilitating a larger step at the initial iteration and finer steps in subsequent iterations to reconstruct detailed information.

6. Conclusion

In this paper, we propose a progressive divide-and-conquer framework for accelerated MRI. We first decompose the subsampling process of the severe degradation in accelerated MRI into a series of moderate degradations. Following this, we provide a detailed derivation of the PDAC reconstruction process, which is subsequently unfolded into an end-to-end trainable network. Each iteration in PDAC is dedicated to recovering partial information within the null space, specifically addressing a particular moderate degradation based on the decomposition. Furthermore, as part of the PDAC iteration, we incorporate the learning of degradation decomposition as an auxiliary task using a degradation predictor and a severity conditioning module. Finally, our extensive experimental results consistently demonstrate the superior performance of the proposed PDAC strategy in both single-coil and multi-coil MRI reconstruction on the fastMRI and Stanford2D FSE datasets.

References

- [1] M. V Afonso, J. M Bioucas-Dias, and M. AT Figueiredo. Fast image recovery using variable splitting and constrained optimization. *IEEE transactions on image processing*, 19(9): 2345–2356, 2010. [3](#), [4](#)
- [2] Hemant K. Aggarwal, Merry P. Mani, and Mathews Jacob. Modl: Model-based deep learning architecture for inverse problems. *IEEE Transactions on Medical Imaging*, 38(2): 394–405, 2019. [2](#)
- [3] Wafa Alghallabi, Akshay Dudhane, Waqas Zamir, Salman Khan, and Fahad Shahbaz Khan. Accelerated mri reconstruction via dynamic deformable alignment based transformer. In *International Workshop on Machine Learning in Medical Imaging*, pages 104–114. Springer, 2023. [2](#)
- [4] Marius Arvinte, Sriram Vishwanath, Ahmed H Tewfik, and Jonathan I Tamir. Deep j-sense: Accelerated mri reconstruction via unrolled alternating optimization. In *Medical Image Computing and Computer Assisted Intervention–MICCAI 2021: 24th International Conference, Strasbourg, France, September 27–October 1, 2021, Proceedings, Part VI 24*, pages 350–360. Springer, 2021. [2](#)
- [5] A. Beck and M. Teboulle. A fast iterative shrinkage-thresholding algorithm for linear inverse problems. *SIAM journal on imaging sciences*, 2(1):183–202, 2009. [2](#)
- [6] Sayantan Bhadra, Varun A Kelkar, Frank J Brooks, and Mark A Anastasio. On hallucinations in tomographic image reconstruction. *IEEE transactions on medical imaging*, 40(11):3249–3260, 2021. [1](#)
- [7] Antoni Buades, Bartomeu Coll, and J-M Morel. A non-local algorithm for image denoising. In *2005 IEEE computer society conference on computer vision and pattern recognition (CVPR’05)*, pages 60–65. Ieee, 2005. [5](#)
- [8] Jing Cheng, Haifeng Wang, Leslie Ying, and Dong Liang. Model learning: Primal dual networks for fast mr imaging. In *Medical Image Computing and Computer Assisted Intervention–MICCAI 2019: 22nd International Conference, Shenzhen, China, October 13–17, 2019, Proceedings, Part III 22*, pages 21–29. Springer, 2019. [1](#)
- [9] Joseph Y. Cheng. Stanford 2d fse. In <http://mridata.org/list?project=Stanford2DFSE>. [6](#), [7](#)
- [10] David L Donoho. Compressed sensing. *IEEE Transactions on information theory*, 52(4):1289–1306, 2006. [1](#)
- [11] Taejoon Eo, Yohan Jun, Taeseong Kim, Jinseong Jang, Ho-Joon Lee, and Dosik Hwang. Kiki-net: cross-domain convolutional neural networks for reconstructing undersampled magnetic resonance images. *Magnetic resonance in medicine*, 80(5):2188–2201, 2018. [7](#), [8](#)
- [12] Zalan Fabian, Berk Tinaz, and Mahdi Soltanolkotabi. Humus-net: Hybrid unrolled multi-scale network architecture for accelerated mri reconstruction. *Advances in Neural Information Processing Systems*, 35:25306–25319, 2022. [2](#), [6](#), [7](#), [8](#)
- [13] Karol Gregor and Yann LeCun. Learning fast approximations of sparse coding. In *Proceedings of the 27th international conference on international conference on machine learning*, pages 399–406, 2010. [2](#)
- [14] Pengfei Guo, Jeya Maria Jose Valanarasu, Puyang Wang, Jinyuan Zhou, Shanshan Jiang, and Vishal M Patel. Over-and-under complete convolutional rnn for mri reconstruction. In *Medical Image Computing and Computer Assisted Intervention–MICCAI 2021: 24th International Conference, Strasbourg, France, September 27–October 1, 2021, Proceedings, Part VI 24*, pages 13–23. Springer, 2021. [6](#), [7](#), [8](#)
- [15] Pengfei Guo, Yiqun Mei, Jinyuan Zhou, Shanshan Jiang, and Vishal M Patel. Reconformer: Accelerated mri reconstruction using recurrent transformer. *IEEE Transactions on Medical Imaging*, 2023. [6](#), [7](#), [8](#)
- [16] Ajil Jalal, Marius Arvinte, Giannis Daras, Eric Price, Alexandros G Dimakis, and Jon Tamir. Robust compressed sensing mri with deep generative priors. *Advances in Neural Information Processing Systems*, 34:14938–14954, 2021. [1](#)
- [17] Yohan Jun, Hyungseob Shin, Taejoon Eo, and Dosik Hwang. Joint deep model-based mr image and coil sensitivity reconstruction network (joint-icnet) for fast mri. In *Proceedings of the IEEE/CVF Conference on Computer Vision and Pattern Recognition*, pages 5270–5279, 2021. [2](#)
- [18] Shengjiang Kong, Weiwei Wang, Xiangchu Feng, and Xixi Jia. Deep red unfolding network for image restoration. *IEEE Transactions on Image Processing*, 31:852–867, 2021. [2](#)
- [19] Jingyun Liang, Jiezhang Cao, Guolei Sun, Kai Zhang, Luc Van Gool, and Radu Timofte. Swinir: Image restoration using swin transformer. In *Proceedings of the IEEE/CVF international conference on computer vision*, pages 1833–1844, 2021. [7](#), [8](#)
- [20] Sajjan Goud Lingala, Yue Hu, Edward DiBella, and Mathews Jacob. Accelerated dynamic mri exploiting sparsity and low-rank structure: k-t slr. *IEEE Transactions on Medical Imaging*, 30(5):1042–1054, 2011. [2](#)
- [21] Ilya Loshchilov and Frank Hutter. Decoupled weight decay regularization. *arXiv preprint arXiv:1711.05101*, 2017. [6](#)
- [22] Michael Lustig, David Donoho, and John M Pauly. Sparse mri: The application of compressed sensing for rapid mr imaging. *Magnetic Resonance in Medicine: An Official Journal of the International Society for Magnetic Resonance in Medicine*, 58(6):1182–1195, 2007. [1](#)
- [23] Michael Lustig, David Donoho, and John M Pauly. Sparse mri: The application of compressed sensing for rapid mr imaging. *Magnetic Resonance in Medicine: An Official Journal of the International Society for Magnetic Resonance in Medicine*, 58(6):1182–1195, 2007. [2](#)
- [24] Chong Mou, Qian Wang, and Jian Zhang. Deep generalized unfolding networks for image restoration. In *Proceedings of the IEEE/CVF Conference on Computer Vision and Pattern Recognition*, pages 17399–17410, 2022. [2](#)
- [25] Matthew J Muckley, Bruno Riemenschneider, Alireza Radmanesh, Sunwoo Kim, Geunu Jeong, Jingyu Ko, Yohan Jun, Hyungseob Shin, Dosik Hwang, Mahmoud Mostapha, et al. Results of the 2020 fastmri challenge for machine learning mr image reconstruction. *IEEE transactions on medical imaging*, 40(9):2306–2317, 2021. [2](#)
- [26] Osvald Nitski, Sayan Nag, Chris McIntosh, and Bo Wang. Cdf-net: Cross-domain fusion network for accelerated mri

- reconstruction. In *International Conference on Medical Image Computing and Computer-Assisted Intervention*, pages 421–430. Springer, 2020. 2
- [27] William Peebles and Saining Xie. Scalable diffusion models with transformers. In *Proceedings of the IEEE/CVF International Conference on Computer Vision*, pages 4195–4205, 2023. 6
- [28] Saiprasad Ravishankar and Yoram Bresler. Mr image reconstruction from highly undersampled k-space data by dictionary learning. *IEEE Transactions on Medical Imaging*, 30(5):1028–1041, 2011. 2
- [29] Saiprasad Ravishankar and Yoram Bresler. Efficient blind compressed sensing using sparsifying transforms with convergence guarantees and application to magnetic resonance imaging. *SIAM Journal on Imaging Sciences*, 8(4):2519–2557, 2015. 1
- [30] Olaf Ronneberger, Philipp Fischer, and Thomas Brox. U-net: Convolutional networks for biomedical image segmentation. In *Medical Image Computing and Computer-Assisted Intervention—MICCAI 2015: 18th International Conference, Munich, Germany, October 5–9, 2015, Proceedings, Part III 18*, pages 234–241. Springer, 2015. 6, 7, 8
- [31] Jo Schlemper, Jose Caballero, Joseph V Hajnal, Anthony Price, and Daniel Rueckert. A deep cascade of convolutional neural networks for mr image reconstruction. In *Information Processing in Medical Imaging: 25th International Conference, IPMI 2017, Boone, NC, USA, June 25–30, 2017, Proceedings 25*, pages 647–658. Springer, 2017. 1, 7, 8
- [32] Anuroop Sriram, Jure Zbontar, Tullie Murrell, Aaron Defazio, C Lawrence Zitnick, Nafissa Yakubova, Florian Knoll, and Patricia Johnson. End-to-end variational networks for accelerated mri reconstruction. In *Medical Image Computing and Computer Assisted Intervention—MICCAI 2020: 23rd International Conference, Lima, Peru, October 4–8, 2020, Proceedings, Part II 23*, pages 64–73. Springer, 2020. 6, 7
- [33] Jonathan I Tamir, Frank Ong, Joseph Y Cheng, Martin Uecker, and Michael Lustig. Generalized magnetic resonance image reconstruction using the berkeley advanced reconstruction toolbox. In *ISMRM Workshop on Data Sampling & Image Reconstruction, Sedona, AZ, 2016*. 7, 8
- [34] Andreas M Tillmann and Marc E Pfetsch. The computational complexity of the restricted isometry property, the nullspace property, and related concepts in compressed sensing. *IEEE Transactions on Information Theory*, 60(2):1248–1259, 2013. 5
- [35] Martin Uecker, Peng Lai, Mark J Murphy, Patrick Virtue, Michael Elad, John M Pauly, Shreyas S Vasanawala, and Michael Lustig. Espirit—an eigenvalue approach to autocalibrating parallel mri: where sense meets grappa. *Magnetic resonance in medicine*, 71(3):990–1001, 2014. 6, 7
- [36] Jeya Maria Jose Valanarasu, Vishwanath A Sindagi, Ilker Hacihaliloglu, and Vishal M Patel. Kiu-net: Towards accurate segmentation of biomedical images using over-complete representations. In *Medical Image Computing and Computer Assisted Intervention—MICCAI 2020: 23rd International Conference, Lima, Peru, October 4–8, 2020, Proceedings, Part IV 23*, pages 363–373. Springer, 2020. 7, 8
- [37] Chong Wang, Rongkai Zhang, Gabriel Maliakal, Saiprasad Ravishankar, and Bihan Wen. Deep reinforcement learning based unrolling network for mri reconstruction. In *2023 IEEE 20th International Symposium on Biomedical Imaging (ISBI)*, pages 1–5. IEEE, 2023. 2
- [38] Bingyu Xin, Meng Ye, Leon Axel, and Dimitris N Metaxas. Fill the k-space and refine the image: Prompting for dynamic and multi-contrast mri reconstruction. In *International Workshop on Statistical Atlases and Computational Models of the Heart*, pages 261–273. Springer, 2023. 2
- [39] Yan Yang, Jian Sun, Huibin Li, and Zongben Xu. Deep admm-net for compressive sensing mri. In *Advances in Neural Information Processing Systems*. Curran Associates, Inc., 2016. 1, 2
- [40] Yan Yang, Na Wang, Heran Yang, Jian Sun, and Zongben Xu. Model-driven deep attention network for ultra-fast compressive sensing mri guided by cross-contrast mr image. In *Medical Image Computing and Computer Assisted Intervention—MICCAI 2020: 23rd International Conference, Lima, Peru, October 4–8, 2020, Proceedings, Part II 23*, pages 188–198. Springer, 2020. 2
- [41] George Yiasemis, Jan-Jakob Sonke, Clarisa Sánchez, and Jonas Teuwen. Recurrent variational network: a deep learning inverse problem solver applied to the task of accelerated mri reconstruction. In *Proceedings of the IEEE/CVF conference on computer vision and pattern recognition*, pages 732–741, 2022. 6
- [42] Jure Zbontar, Florian Knoll, Anuroop Sriram, Tullie Murrell, Zhengnan Huang, Matthew J. Muckley, Aaron Defazio, Ruben Stern, Patricia Johnson, Mary Bruno, Marc Parente, Krzysztof J. Geras, Joe Katsnelson, Hersh Chandarana, Zizhao Zhang, Michal Drozdal, Adriana Romero, Michael Rabbat, Pascal Vincent, Nafissa Yakubova, James Pinkerton, Duo Wang, Erich Owens, C. Lawrence Zitnick, Michael P. Recht, Daniel K. Sodickson, and Yvonne W. Lui. fastMRI: An open dataset and benchmarks for accelerated MRI, 2018. 6, 7
- [43] Kai Zhang, Luc Van Gool, and Radu Timofte. Deep unfolding network for image super-resolution. In *Proceedings of the IEEE/CVF conference on computer vision and pattern recognition*, pages 3217–3226, 2020. 1, 2
- [44] Hao Zheng, Faming Fang, and Guixu Zhang. Cascaded dilated dense network with two-step data consistency for mri reconstruction. *Advances in Neural Information Processing Systems*, 32, 2019. 1
- [45] Hongyi Zheng, Hongwei Yong, and Lei Zhang. Unfolded deep kernel estimation for blind image super-resolution. In *European Conference on Computer Vision*, pages 502–518. Springer, 2022. 1, 2
- [46] Bo Zhou and S Kevin Zhou. Dudornet: Learning a dual-domain recurrent network for fast mri reconstruction with deep t1 prior. In *Proceedings of the IEEE/CVF Conference on Computer Vision and Pattern Recognition*, pages 4273–4282, 2020. 2